

LETTERS

The unexpected origin of plasmaspheric hiss from discrete chorus emissions

Jacob Bortnik¹, Richard M. Thorne¹ & Nigel P. Meredith²

Plasmaspheric hiss¹ is a type of electromagnetic wave found ubiquitously in the dense plasma region that encircles the Earth, known as the plasmasphere². This important wave is known to remove^{3–5} the high-energy electrons that are trapped along the Earth's magnetic field lines⁶, and therefore helps to reduce the radiation hazards to satellites and humans in space. Numerous theories to explain the origin of hiss have been proposed over the past four decades, but none have been able to account fully for its observed properties. Here we show that a different wave type called chorus^{7,8}, previously thought to be unrelated to hiss, can propagate into the plasmasphere from tens of thousands of kilometres away, and evolve into hiss. Our new model naturally accounts for the observed frequency band of hiss, its incoherent nature, its day–night asymmetry in intensity, its association with solar activity and its spatial distribution. The connection between chorus and hiss is very interesting because chorus is instrumental in the formation of high-energy electrons outside the plasmasphere⁹, whereas hiss depletes these electrons at lower equatorial altitudes^{3,4}.

Early spacecraft observations beginning in the late 1960s, of wide-band electromagnetic noise at frequencies below a few kilohertz established the presence of a steady, incoherent noise band in the frequency range between ~ 200 Hz and ~ 1 kHz (refs 7, 8 and 10). This emission was named plasmaspheric hiss¹ because of its unstructured nature, spectral resemblance to audible hiss, and confinement to the plasmasphere. Hiss occurs at all local times, but intensities are strongest on the day side^{1,10,11}, and further increase when geomagnetic activity (such as storms and substorms, ultimately driven by solar activity) is increased¹¹. There have been a number of different hypotheses attempting to explain the origin of hiss¹² (see Supplementary Information for further discussion), but only two have emerged as the most likely candidates: (1) the *in situ* growth and amplification of background electromagnetic turbulence, driven by unstable energetic electron populations^{1,13}, and (2) the evolution of a spectrum of electromagnetic waves injected into the plasmasphere by terrestrial lightning strikes, into the observed hiss band^{14–17}. However, there are observational difficulties with both leading models for the origin of hiss. Typical wave growth rates inside the plasmasphere are too modest¹³ to generate the observed emissions. Alternatively, if plasmaspheric hiss originated from lightning, the emissions would be stronger over the continents than over the oceans because lightning activity is more prevalent over land. A recent study¹⁸ of the geographic association of plasmaspheric emissions above 3 kHz led to substantial controversy^{19,20}, and a more extensive study²¹ showed that hiss below 2 kHz, where the emission power is strongest, has no correlation with landmass. In addition, a lightning source of hiss cannot account for the pronounced association of wave intensities with geomagnetic activity. Clearly, an alternative

explanation is required that is theoretically viable and can simultaneously account for all the observed features of hiss.

Figure 1b shows a dynamic spectrogram of an electromagnetic emission known as chorus^{7,8,22}, which, unlike hiss, occurs in the unstable region outside the plasmasphere. The intensity and spectral characteristics of chorus are very different to those of hiss (Fig. 1c). Chorus wave power is typically greater than that of hiss^{1,11,23}, and consists of discrete spectral features, which rise at a rate of the order of 1 kHz s^{-1} over a well-defined frequency band controlled by the equatorial electron gyrofrequency (f_{ce} , defined as the frequency with which electrons gyrate about the Earth's magnetic field line, and which is proportional to the magnetic field strength). Chorus typically occurs in two frequency bands: a lower, more intense, band in the range $\sim 0.1\text{--}0.45f_{ce}$, and an upper band at $\sim 0.5\text{--}0.7f_{ce}$. In contrast, hiss remains in a roughly constant frequency band of $\sim 0.2\text{--}1$ kHz throughout the entire plasmasphere.

The propagation of chorus has been modelled as shown in Fig. 1a, using numerical ray tracing for a set of rays initiated at the geomagnetic equator, consistent with observations²². The rays are injected at $L = 5$, where L is the distance in Earth radii ($1 R_E = 6,370$ km) from the centre of the Earth to the equatorial crossing of a given magnetic field line, at the lower end of the chorus frequency spectrum, $0.1f_{ce}$, corresponding to a frequency of 704 Hz. Each ray is initiated with a slightly different wave normal angle ψ_0 (defined as the angle between the Earth's magnetic field, and the normal to the plane of the wave, with negative angles pointed towards the Earth), and colour-coded accordingly. The damping experienced by each ray is accurately calculated²³, and each ray is plotted until it decays to 1% of its initial power.

The rays exhibit a variety of behaviours. Those rays with ψ_0 near -70° or $+20^\circ$ are completely damped before they reach high latitudes (for example, $\lambda \approx 50^\circ$), while the rays with $\psi_0 \approx -25^\circ$ to $+10^\circ$ (day side) magnetospherically reflect at high latitudes, and propagate away from the Earth, probably contributing to an emission previously reported as extremely low frequency hiss^{8,24}. However, a key range of rays with $\psi_0 \approx -30^\circ$ to -60° (day side), magnetospherically reflect towards lower L ²⁵, and propagate into the plasmasphere. Once inside the plasmasphere, the damping rate is dramatically reduced owing to the high cold electron density, and low electron fluxes which produce the damping. The rays internally reflect many times before being completely damped, and in so doing, fill the plasmasphere with wave energy down to $L \approx 1.6$, consistent with observations¹ (see Supplementary Information for a detailed ray path and discussion). Each ray has a slightly different entry point into the plasmasphere, so the chorus rays which propagated coherently outside the plasmasphere become completely randomized after only one or two internal reflections inside the plasmasphere, leading to the incoherent nature of hiss. Also clearly evident is the dramatic

¹Department of Atmospheric and Oceanic Sciences, University of California, Los Angeles, 405 Hilgard Avenue, Los Angeles, California 90095, USA. ²British Antarctic Survey, Natural Environment Research Council, Madingley Road, Cambridge, CB3 0ET, UK.

difference between day and night in the access of rays into the plasmasphere, due primarily to the different electron fluxes responsible for the damping.

To quantify the plasmaspheric access of chorus, rays were traced for different initial values of L , ψ_0 and frequency, and the lifetime τ (defined to be the time taken for the ray to reach 1% of its initial power) was recorded. The results (shown in Fig. 2) can be interpreted as follows: rays that are completely damped before they reach high latitudes typically have $\tau < 1$ s, those that reflect and propagate to higher latitudes typically have $\tau < 5$ s, but rays that enter the plasmasphere have much longer lifetimes. A certain set of rays, marked by the letter I, originating at $L \approx 4.5\text{--}6.5$, have lifetimes exceeding 30 s, and coincidentally have frequencies in the range $\sim 0.2\text{--}1$ kHz, identical to

the observed hiss spectrum. On the night side, fewer waves are able to access the plasmasphere, and those that do have much shorter lifetimes, typically $\tau \approx 10$ s. As the frequency of the source population of chorus is increased (day side in Fig. 2c and e; night side in Fig. 2d and f), access into the plasmasphere becomes more restricted, and τ is lowered to less than 10 s, accounting for the reduced intensities of hiss above 1 kHz, and the weaker emissions observed on the night side. The power spectral intensity of those waves that access the plasmasphere is enhanced, owing to the multiple magnetospheric reflections and the reduced magnetospheric volume occupied by hiss compared to that occupied by chorus. Consequently, only a small fraction of the chorus wave power needs to leak into the plasmasphere to account for typical hiss intensities. Interestingly, we also note in Fig. 1a that

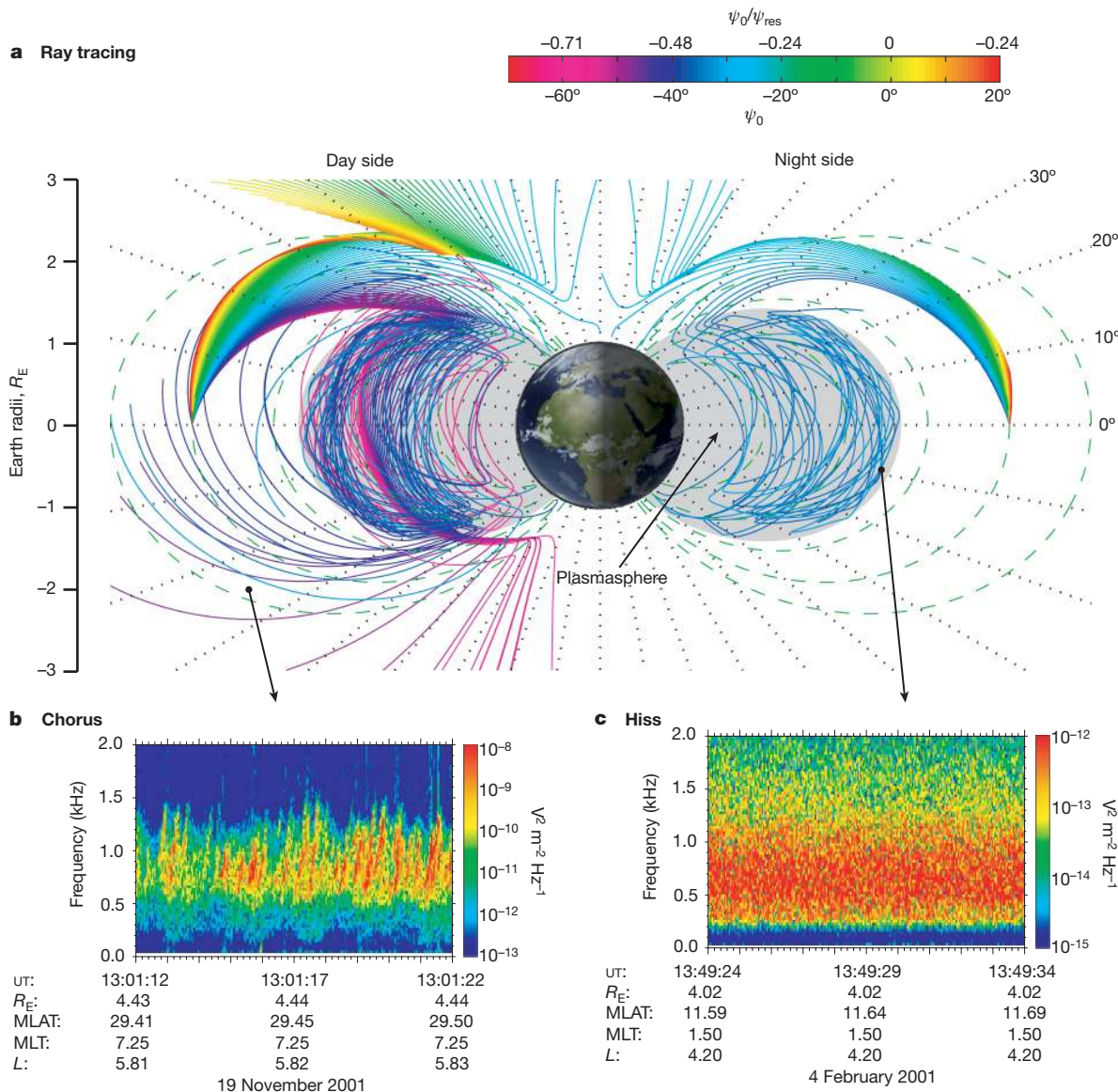


Figure 1 | Evolution of chorus into plasmaspheric hiss. **a**, A schematic of the near-Earth space environment, with the grey regions indicating the typical location of the dense plasmasphere. A set of 91 rays is launched from the geomagnetic equator (that is, $\lambda = 0^\circ$) at $L = 5$, with $f = 0.1f_{ce}$ (704 Hz), in the wave normal range -70° to $+20^\circ$, at every 1° . Each ray is traced until its power decreases to 1% of its initial value, at which point the ray is terminated. Chorus originating with a different frequency and starting location will have a similar set of ray paths, which will merge together into an incoherent emission to fill the outer plasmasphere with hiss. **b**, A 10-s-long spectrogram showing the intensity of a typical series of rising chorus elements, as a function of frequency and time, observed by the Wideband

instrument on the Cluster II satellite on the day side outside the plasmasphere. **c**, A similar 10-s-long spectrogram showing plasmaspheric hiss intensity, on the night side inside the plasmasphere. There is a sharp lower frequency cut-off at ~ 200 Hz, and a more gradual upper frequency cut-off at ~ 1 kHz, and no apparent structure in the spectrum. The abscissas shown represent: UT, Universal time; MLT, magnetic local time, which is the local time of equatorial crossing of the magnetic field-line passing through the satellite, and can be slightly different to the actual local time; and MLAT, magnetic latitude, the latitude of CRRES relative to the geomagnetic equator.

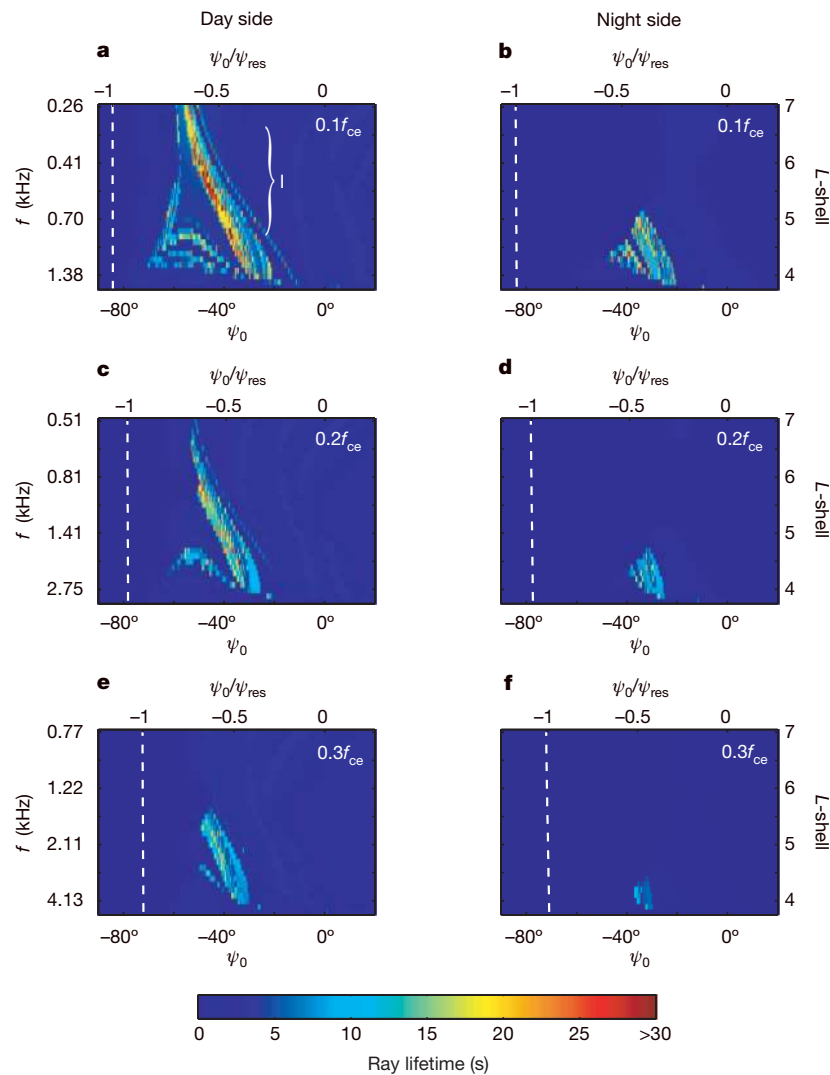


Figure 2 | Penetration characteristics of chorus rays. Each pixel represents a single chorus ray, initiated at the geomagnetic equator at the location L and the wave normal ψ_0 shown. Each chorus ray is ray-traced until its power decreases to 1% of its initial value, and the time is recorded, and displayed using the colour scale at the bottom of the figure. The day side and night side cold plasma distribution is modelled after ref. 28, the field is assumed to be dipolar, and the suprathermal flux distribution used in the calculation of Landau damping outside the plasmasphere is obtained from the CRRES, following the methodology of ref. 23, taking the distribution to be MLT and

some of the chorus rays pass through the plasmasphere, exit and return to the outer magnetosphere. Such emissions have been observed and referred to as exo-hiss in past studies¹ but their origin appears to be chorus.

An observation of hiss and chorus waves from the Combined Release and Radiation Effects Satellite (CRRES) is shown in Fig. 3. During the inbound leg of the orbit (after $\sim 11:00$ UT), the satellite travels from higher to lower L and enters the plasmasphere on the day side. Although individual chorus elements cannot be distinguished on this timescale, the frequency band of chorus clearly follows the equatorial gyrofrequency, increasing in frequency as the satellite moves to lower L , and remaining confined roughly to the band $\sim 0.1\text{--}0.45f_{ce}$. On entering the plasmasphere, the chorus emissions are abruptly cut off at $\sim 14:40$ UT, and are replaced by the typical plasmaspheric hiss band, which has a peak intensity near the outer boundary of the plasmasphere and becomes weaker closer to the Earth. Many of the features discussed above are evident in this plot, including the increased intensity of hiss on the day side versus the

L -dependent. Inside the plasmasphere, the flux distribution from ref. 29 is assumed. **a–f**, Each panel shows chorus ray lifetimes, for frequencies $ff_{ce} = 0.1, 0.2$ and 0.3 as shown, normalized to the electron gyrofrequency, with the actual wave frequency f associated with the ray's initial L value. ψ_0 normalized to the resonance-cone angle ψ_{res} , beyond which propagation in the cold-plasma whistler-mode is not possible, is also shown. Rays with lifetimes over 5 s have all entered and remained in the plasmasphere (Fig. 1a), with some rays reaching lifetimes well over 50 s.

night side, and the approximate location of the chorus source region, which is believed to leak into the plasmasphere and evolve into hiss (marked by the letter 'S' in Fig. 3), indicating that the rays responsible for the most intense portion of the hiss spectrum are generated well outside the plasmasphere, and not adjacent to it. Also visible is exo-hiss, at $\sim 14:00\text{--}14:40$, $f \approx 0.2\text{--}0.5$ kHz, outside the plasmasphere, which is believed to have leaked out, as described above. The upper frequency cut-off of both the hiss and chorus waves near the plasmasphere boundary shows a very close correspondence, suggesting that it is these higher-frequency chorus waves that have leaked into the plasmasphere and evolved into the hiss spectrum, but at much lower intensities than the components at less than 1 kHz, as is clearly reproduced in our simulations.

The present modelling study is the first to link chorus to the origin of plasmaspheric hiss. Much detailed modelling remains to be done in this area, but our results naturally account for the essential features of hiss, such as the observed frequency spectrum, its incoherent nature, the day–night asymmetry in intensity, the distribution in L ,

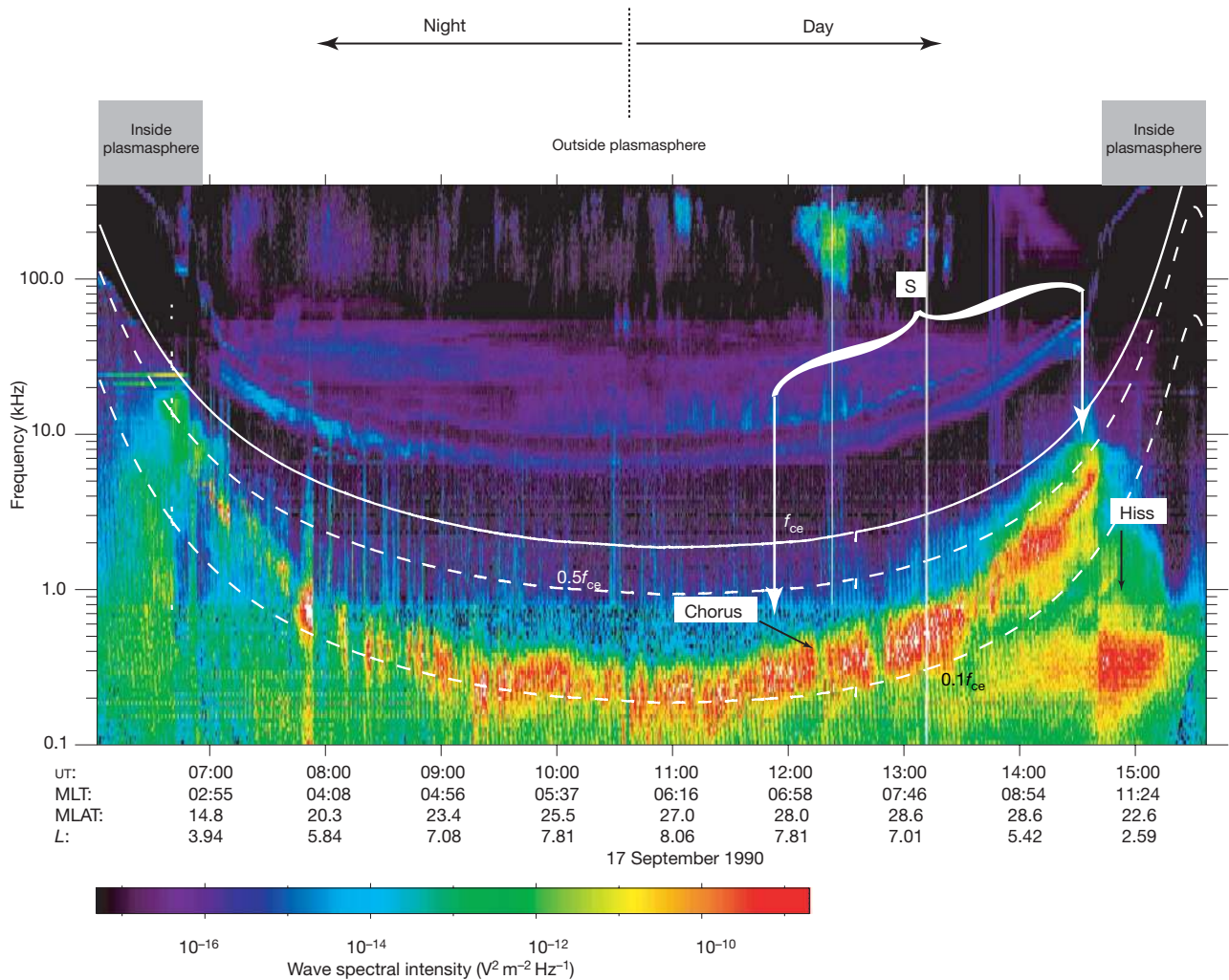


Figure 3 | CRRES satellite data showing chorus and hiss emissions. Survey plot (~9 h) of the wave spectral intensity for orbit 130 from the CRRES Plasma Wave Experiment. The region marked “S” is the source region of chorus from which waves propagate into the plasmasphere and evolve into hiss. We note that there is not a perfect correspondence between the observed chorus and the hiss, because the CRRES satellite was changing its

local time rapidly, observing the chorus on the dawn side of the Earth, and the hiss close to noon, so the chorus waves that evolve into the hiss shown would have been produced on the day side, and are different from those shown in the spectrogram (though they would have been qualitatively very similar). The L value of CRRES is calculated using the Olson–Pfitzer tilt-dependent static model³⁰ and the IGRF 85 model.

the geomagnetic control^{11,26,27}, as well as other ancillary features, such as exo-hiss and extremely low frequency hiss. We thus contend that chorus waves are the dominant source of plasmaspheric hiss.

Received 1 May 2007; accepted 16 January 2008.

- Thorne, R. M., Smith, E. J., Burton, R. K. & Holzer, R. E. Plasmaspheric hiss. *J. Geophys. Res.* **78**, 1581–1595 (1973).
- Carpenter, D. L. & Park, C. G. What ionospheric workers should know about the plasmapause/plasmasphere. *Rev. Geophys.* **11**, 133–154 (1973).
- Lyons, L. R., Thorne, R. M. & Kennel, C. F. Pitch-angle diffusion of radiation belt electrons within the plasmasphere. *J. Geophys. Res.* **77**, 3455–3474 (1972).
- Abel, R. W. & Thorne, R. M. Electron scattering loss in Earth’s inner magnetosphere. 1: Dominant physical processes. *J. Geophys. Res.* **103**, 2385–2396 (1998).
- Lyons, L. R. & Thorne, R. M. Equilibrium structure of radiation belt electrons. *J. Geophys. Res.* **78**, 2142–2149 (1973).
- Van Allen, J. A. in *Discovery of the Magnetosphere* (eds Gillmor, C. S. & Spreiter, J. R.) *History of Geophysics* Vol. 7 235–251 (American Geophysical Union, Washington DC, 1997).
- Dunckel, N. & Helliwell, R. A. Whistler mode emissions on the Ogo 1 satellite. *J. Geophys. Res.* **74**, 6371–6385 (1969).
- Russell, C. T., Holzer, R. E. & Smith, E. J. OGO 3 observations of ELF noise in the magnetosphere: 1. Spatial extent and frequency of occurrence. *J. Geophys. Res.* **74**, 755–777 (1969).
- Horne, R. B. *et al.* Timescales for radiation belt electron acceleration by whistler mode chorus waves. *J. Geophys. Res.* **111**, A03225, doi:10.1029/2004JA010811 (2005).
- Taylor, W. W. L. & Gurnett, D. A. The morphology of VLF emissions observed with the Injun 3 satellite. *J. Geophys. Res.* **73**, 5615–5626 (1968).
- Meredith, N. P. *et al.* Substorm dependence of plasmaspheric hiss. *J. Geophys. Res.* **109**, A06209, doi:10.1029/2004JA010387 (2004).
- Hayakawa, M. & Sazhin, S. S. Mid-latitude and plasmaspheric hiss: a review. *Planet. Space Sci.* **40**, 1325–1338 (1992).
- Church, S. R. & Thorne, R. M. On the origin of plasmaspheric hiss: ray path integrated amplification. *J. Geophys. Res.* **88**, 7941–7957 (1983).
- Sonwalkar, V. S. & Inan, U. S. Lightning as an embryonic source of VLF hiss. *J. Geophys. Res.* **94**, 6986–6994 (1989).
- Draganov, A. B., Inan, U. S., Sonwalkar, V. S. & Bell, T. F. Magnetospherically reflected whistlers as a source of plasmaspheric hiss. *J. Geophys. Res.* **19**, 233–236 (1992).
- Bortnik, J., Inan, U. S. & Bell, T. F. Frequency-time spectra of magnetospherically reflecting whistlers in the plasmasphere. *J. Geophys. Res.* **108** (A1), 1030, doi:10.1029/2002JA009387 (2003).
- Bortnik, J., Inan, U. S. & Bell, T. F. Energy distribution and lifetime of magnetospherically reflecting whistlers in the plasmasphere. *J. Geophys. Res.* **108** (A5), 1199, doi:10.1029/2002JA009316 (2003).
- Green, J. L. *et al.* On the origin of whistler mode radiation in the plasmasphere. *J. Geophys. Res.* **110**, A03201, doi:10.1029/2004JA010495 (2005).
- Thorne, R. M., Horne, R. B. & Meredith, N. P. Comment on “On the origin of whistler mode radiation in the plasmasphere” by Green *et al.* *J. Geophys. Res.* **111**, A09210, doi:10.1029/2005JA011477 (2006).
- Green, J. L. *et al.* Reply to ‘Comment on “On the origin of whistler mode radiation in the plasmasphere” by Green *et al.*’ *J. Geophys. Res.* **111**, A09211, doi:10.1029/2006JA011622 (2006).

21. Meredith, N. P. *et al.* Origins of plasmaspheric hiss. *J. Geophys. Res.* **111**, A09217, doi:10.1029/2006JA011707 (2006).
22. Burtis, W. J. & Helliwell, R. A. Magnetospheric chorus: occurrence patterns and normalized frequency. *Planet. Space Sci.* **24**, 1007–1024 (1976).
23. Bortnik, J., Thorne, R. M. & Meredith, N. P. Modeling the propagation characteristics of chorus using CRRES suprathermal electron fluxes. *J. Geophys. Res.* **112**, A08204, doi:10.1029/2006JA012237 (2007).
24. Santolik, O. *et al.* Propagation of whistler mode chorus to low altitudes: Spacecraft observations of structured ELF hiss. *J. Geophys. Res.* **111**, A10208, doi:10.1029/2005JA011462 (2006).
25. Thorne, R. M. & Kennel, C. F. Quasi-trapped VLF propagation in the outer magnetosphere. *J. Geophys. Res.* **72**, 857–870 (1967).
26. Smith, E. J., Frandsen, A. M. A., Tsurutani, B. T., Thorne, R. M. & Chan, K. W. Plasmaspheric hiss intensity variations during magnetic storms. *J. Geophys. Res.* **79**, 2507–2510 (1974).
27. Thorne, R. M., Smith, E. J., Fiske, K. J. & Church, S. R. Intensity variation of ELF hiss and chorus during isolated substorms. *Geophys. Res. Lett.* **1**, 193–196 (1974).
28. Carpenter, D. L. & Anderson, R. R. An ISEE/whistler model of equatorial electron density in the magnetosphere. *J. Geophys. Res.* **97** (A2), 1097–1108 (1992).
29. Bell, T. F., Inan, U. S., Bortnik, J. & Scudder, J. D. The Landau damping of magnetospherically reflected whistlers within the plasmasphere. *Geophys. Res. Lett.* **29**, 15, doi:10.1029/2002GL014752 (2002).
30. Olson, W. P. & Pfitzer, K. *Magnetospheric Magnetic Field Modelling*. Annual Scientific Report, AFOSR Contract No. F44620–75-c-0033 (1977).

Supplementary Information is linked to the online version of the paper at www.nature.com/nature.

Acknowledgements J.B. acknowledges support from the National Science Foundation's (NSF) Geospace Environment Modeling (GEM) post-doctoral award and NASA, and R.M.T. acknowledges support from an NSF GEM grant. N.P.M. acknowledges support from the Natural Environment Research Council, UK. We thank Roger R. Anderson for provision of the CRRES plasma wave data used in this study.

Author Contributions J.B. performed all the calculations shown in the paper, wrote the manuscript and Supplementary Information section, and composed all the figures. R.M.T. provided consultation on the theoretical aspects of the work and manuscript writing. N.P.M. provided global models of CRRES/LEPA data used in the Landau damping calculations, the dynamic spectrogram shown in Fig. 3, and input into the manuscript writing.

Author Information Reprints and permissions information is available at www.nature.com/reprints. Correspondence and requests for materials should be addressed to J.B. (jbortnik@gmail.com).